Received: 29 July 2024, Revised: 24 September 2024, Accepted: 26 September 2024, Published: 30 September 2024, Publisher: UTP Press, Creative Commons: CC BY 4.0
(The winner from UTP Engineering Scientific Writing Competition 2024)

IMPACT OF MIXING METHODS AND CONCENTRATIONS ON CORROSION RESISTANCE OF SMART COATING WITH BENZOTRIAZOLE-LOADED HALLOYSITE NANOTUBES

Norshafiera Richard @ Iran[1*], Puteri Sri Melor Megat Yusoff[1], Nuur Fahanis Che Lah[1], Muhammad Yasir[2]

[1]Department of Materials Engineering, Universiti Teknologi Petronas, Malaysia
[2]Department of Mechanical Engineering, Wah Engineering College, Pakistan

*E-mail: norshafiera_20000210@utp.edu.my

ABSTRACT

The oil and gas industry faces significant challenges due to pipeline corrosion, resulting in substantial economic losses and safety risks. This study investigates the effectiveness of smart coatings containing varying concentrations of benzotriazole-loaded halloysite nanotubes (BTA-HNT) and boiled linseed oil microcapsules (MCs) in mitigating corrosion and to investigate the impact of different mixing techniques on the performance of these coatings. Epoxy coatings incorporating BTA-HNT and MCs were applied to carbon steel substrates in concentrations of 10 wt%, 15 wt%, and 20 wt%. Two mixing methods, magnetic stirring and sonication, were assessed for their ability to disperse the microcapsules effectively. Characterisation techniques, including FTIR, EDX, and particle size analysis, confirmed successful encapsulation and uniform distribution of the microcapsules. Electrochemical Impedance Spectroscopy (EIS) and scratch tests revealed that coatings with 15 wt% BTA-HNT and MCs, prepared using sonication, provided superior long-term corrosion protection and self-healing capabilities. Additionally, adhesion tests demonstrated that sonicated samples maintained stronger bonding. These findings highlight the crucial role of microcapsule concentration and mixing techniques in optimising the performance of self-healing epoxy coatings, offering promising solutions for enhanced durability and protection in pipeline infrastructure.

Keywords: *Adhesion test, corrosion protection, self-healing, smart coatings, magnetic stirring, sonication*

INTRODUCTION

The integrity of pipeline infrastructure is crucial for safe and efficient oil and gas transportation. However, these pipelines are continuously exposed to harsh environmental conditions and aggressive agents that make them prone to corrosion. This susceptibility results in significant public safety risks and substantial economic losses due to leaks, repairs, and replacements. Corrosion is an important issue, costing the oil and gas industry approximately US$1,372 billion annually, including US$589 million in surface pipeline and facility costs, US$463 million in downhole tubing, and US$320 million in corrosion-related capital expenditures [1]. Traditional methods, such as cathodic protection and external protective coatings, provide some relief but have limitations. Cathodic protection requires constant monitoring and adjustments, while coatings, though initially effective, are prone to damage and lack self-repair capabilities, necessitating frequent inspections and costly repairs [2].

To address these challenges, self-healing coatings have emerged as a promising solution to enhance the durability and performance of protective coatings for pipelines. Smart coatings are designed to initiate their repair mechanism when the coating's integrity is compromised. When damaged, the encapsulated healing agent (e.g., linseed oil) is released from BTA-HNT microcapsules, filling the cracks through capillary action. The linseed oil then polymerises in the presence of atmospheric oxygen or a chemical catalyst within

another type of microcapsule, effectively sealing the crack and restoring the protective barrier of the coating [3]. This self-healing system significantly reduces the need for manual inspections and repairs, potentially leading to considerable cost savings over the pipeline's lifespan [4].

Despite these advancements, corrosion remains a persistent threat, causing the degradation of steel structures and concrete, resulting in significant economic losses. Existing microcapsule self-healing coating solutions, which incorporate linseed oil, benzotriazole (BTA) corrosion inhibitor, and halloysite nanotubes (HNTs), show promise but require further improvement. Knowledge gaps include the effects of different mixing strategies on incorporating BTA-HNT microcapsules into the epoxy coating and the need to enhance the coating system's repair ability by investigating the impact of various concentrations of BTA-HNT microcapsules [5]-[6]. Developing a dual-functional coating with autonomous self-healing and robust anti-corrosive capabilities remains a significant challenge [7].

Corrosion Challenges in Pipeline

The story of combating corrosion in oil and gas pipelines is one of continuous innovation and discovery. The journey begins with understanding the pervasive corrosion issue, influenced by environmental conditions, fluid composition, and operating loads. Perez [1] has delved into the complexities of microbiologically influenced corrosion (MIC), where sulfate-reducing bacteria (SRB) accelerate metal degradation by producing hydrogen sulfide. This microbial activity forms localised pits and biofilms that significantly weaken pipeline integrity, posing a persistent challenge to engineers and scientists [8]. Recognising the limitations of traditional corrosion prevention methods, the scientific community has turned to developing self-healing coatings [9].

Development of Self-Healing Coatings

Self-healing coatings offer a promising advancement by initiating autonomous repair mechanisms when damage occurs, such as microcracks that can lead to significant integrity issues. The encapsulation of healing agents like linseed oil within the coatings can autonomously seal damages, thus maintaining the coating's integrity and extending the pipeline's operational lifespan [10]. The work of Bi et al. [11] marks a significant milestone in this journey. By encapsulating linseed oil in microcapsules, they created coatings that could effectively seal defects. Their research revealed that scratches up to 300 μm deep could be fully repaired when the concentration of linseed oil microcapsules exceeded 15 wt%, showcasing the potential of self-healing materials in extending the service life of pipelines.

Role of Microcapsules and Nanotubes in Enhancing Coating Efficacy

The exploration of HNTs as carriers for corrosion inhibitors like BTA represents another leap forward [12]-[13]. Njoku et al. [14] demonstrated that HNTs, with their unique tubular structure, could efficiently encapsulate and release inhibitors. This breakthrough showed that coatings incorporating HNTs exhibited significantly improved corrosion resistance, offering a durable solution for protecting metal surfaces from environmental damage. Sun et al. [15] further advanced the field by integrating BTA with HNTs to enhance the self-healing properties of coatings. Their findings indicated that BTA-loaded HNT microcapsules provided a robust barrier against corrosion. The controlled release mechanism of BTA from HNTs proved effective under various pH conditions, ensuring long protection for carbon steel substrates used in pipelines [16]-[18].

Advanced Techniques for Coating Application

The effectiveness of self-healing coatings is also influenced by the application techniques that distribute the microcapsules within the coating matrix [19]. Kurt Çömlekçi and Ulutan [6] explored the effects of different methods, comparing sonication and stirring. Their studies revealed that sonication, by producing finer and more uniformly distributed particles, significantly enhanced the coating's performance. This technique improved the bonding between microcapsules and the epoxy resin, resulting in superior mechanical properties and corrosion resistance [20]-[21].

Concentration of Microcapsules in Coating Performance

The concentration of microcapsules within the self-healing coatings is critical for achieving optimal performance. The varying concentration of microcapsules affects the mechanical properties and self-healing efficiency of the coatings [22]-[23]. Liu et al. [24] contributed to the storyline by optimising the concentration of microcapsules within the coating

matrix. Their research found that a concentration of 15 wt% offered the best balance between corrosion resistance and self-healing capabilities, allowing scratches to be effectively restored within 24 hours. However, Li et al. [2] found that 10 wt% was the optimal concentration for achieving exceptional corrosion resistance and self-healing. This contrast in findings highlights the importance of precise formulation in achieving optimal performance.

Future Research Direction and Gaps

Despite the progress in developing self-healing coatings, there remains a significant gap in understanding microcapsules' optimal concentrations and distributions for maximal efficacy [25]-[26]. Further research is needed to explore these variables in real-world conditions to fully harness the potential of self-healing coatings in the oil and gas industry. This exploration is essential for transitioning laboratory findings into practical applications that can significantly mitigate the corrosion challenges faced by the industry.

METHODOLOGY

Materials

The materials and chemicals required for this study vary across the different stages of smart coating preparation. For microcapsule preparation, urea and formaldehyde are used as the primary shell components, with resorcinol as a cross-linker. Ammonium chloride acts as a hardener, and polyvinyl alcohol (PVA) solution forms the aqueous phase. To prepare BTA-loaded HNT, dry HNT particles are mixed with a saturated BTA solution, acetone, and ultrapure water. Additionally, Copper (II) Sulfate ($CuSO_4$) is used. The materials used to synthesise the smart coating include epoxy resin and a curing agent. The carbon steel substrates used are dimensions of 15 mm × 7.5 mm × 0.5 mm.

Preparation of Coating Additives

The preparation of microcapsules and BTA-loaded HNT involves meticulous steps to ensure effective encapsulation and functionality [27]-[28]. Initially, microcapsules are synthesised by combining 3 g urea, 0.3 g resorcinol, and 0.3 g ammonium chloride in 1000 mL of 1 wt.% polyvinyl alcohol (PVA) solution, adjusting the pH to 3.2. A self-healing agent is added, stirring the mixture at 1000 rpm to create an emulsion. Subsequently, 8.3 mL of formaldehyde is added dropwise, and the reaction is maintained at 55°C for 10 hours to form a thick shell around the microcapsules. Post-reaction, the microcapsules are collected by centrifugation, washed with deionised water, and dried at 150°C, as depicted in Figure 1.

In parallel, BTA-HNT is prepared by mixing 3 grams of dry HNT particles with a saturated BTA solution in acetone. This mixture is then evacuated in a vacuum jar, repeating the process three times to optimise BTA loading. After evacuation, the product is centrifuged, rinsed, and dried. Copper ions are introduced to control the release of BTA by immersing the HNTs in a $CuSO_4$ solution and stirring for 60 seconds, as shown in Figure 2. These preparation steps are crucial for ensuring that the coating additives can deliver effective corrosion resistance and self-healing properties.

Coating Procedure

The preparation of the metal surfaces and the application of the smart coating are critical steps in ensuring the effectiveness of the corrosion prevention and self-healing properties of the coatings. Initially, carbon steel panels, each 0.5 mm thick with a surface

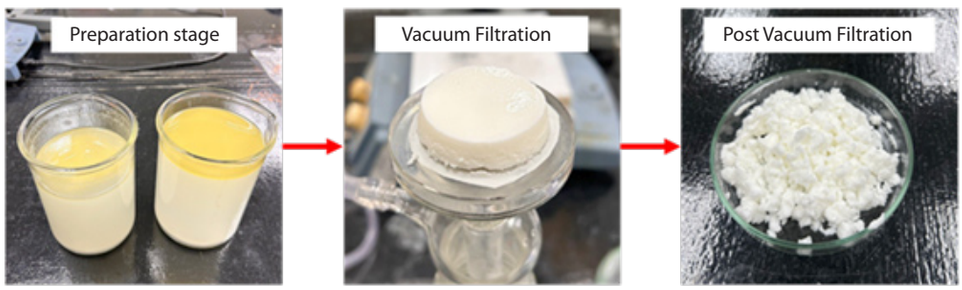

Figure 1 Synthesised of microcapsules

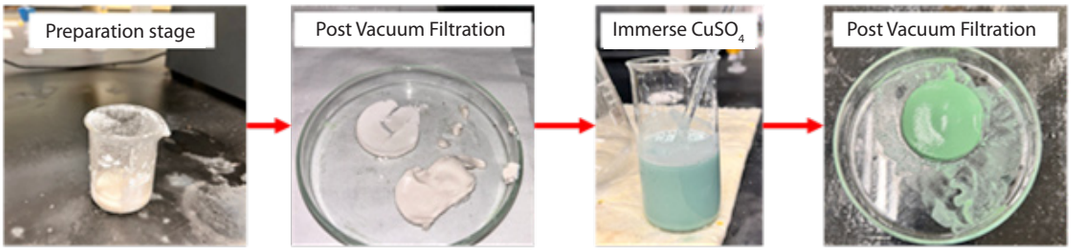

Figure 2 Preparation of BTA-HNT

area of 15 mm × 7.5 mm, were prepared by sandblasting and abrading with 400-grade wet abrasive paper to remove rust, as shown in Figure 3. The surfaces were then thoroughly rinsed with distilled water, degreased with acetone, and left to air dry to ensure a clean substrate for coating application.

For the smart coating preparation, two different mixing techniques were employed to incorporate varying concentrations of BTA-HNT and MCs into the epoxy resin, as detailed in the accompanying study documentation (Table 1). A mixture consisting of 5.0 g of epoxy resin, HNTs loaded with BTA, and specified concentrations of microcapsules containing a self-healing agent was first combined. After adding 1.25 g of curing agent, the mixture was stirred for 5 minutes and mixed for an additional 10 minutes to achieve a uniform dispersion. This homogeneous coating mixture was then applied to the prepared steel substrates to a wet thickness of 500 µm. To ensure consistency and homogeneity in the coating thickness, the required weight of the mixture was calculated based on the dimensions of the substrate. Following this calculation, the coating was applied using an ice cream stick, allowing for uniform distribution across the surface. The samples underwent a curing process for 24 hours, resulting in a robust final dry thickness of 150 µm, as

Table 1 Sample coding for a coating system

Concentration of BTA-HNT and MCs	Mixing Technique	Samples	Label
Epoxy Coating	Stirring	S1	EP
10wt%	Stirring	S2	0.1 St
15 wt%	Stirring	S3	0.15 St
20 wt%	Stirring	S4	0.2 St
15 wt%	Sonication	S5	0.15 Sn

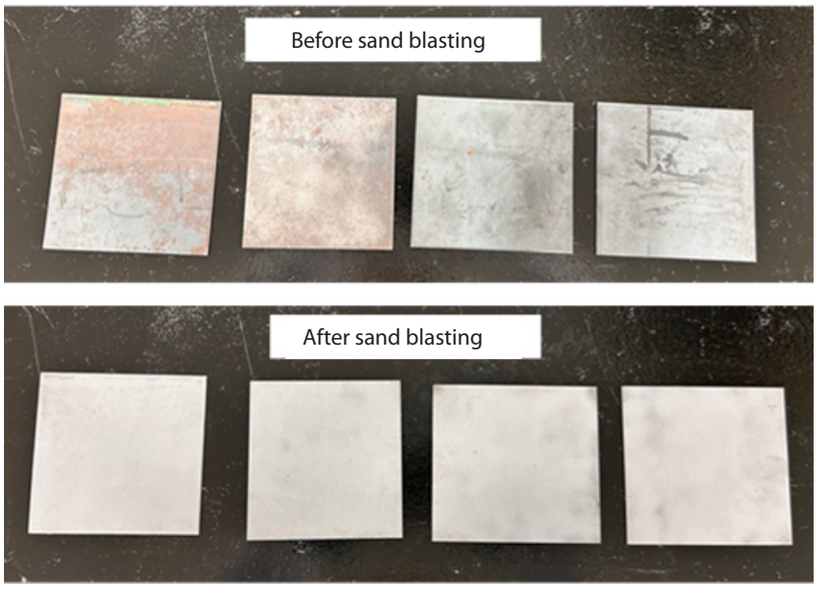

Figure 3 Sample surfaces before and after sandblasted

measured using an elcometer thickness gauge. This comprehensive preparation process aims to enhance the coatings' structural integrity and functionality.

Characterisation of BTA-HNT Microcapsules

Fourier Transform Infrared (FTIR) spectroscopy was conducted on BTA, HNT, and boiled linseed oil to confirm their chemical composition and successful encapsulation in BTA-HNT and MCs, which is vital for assessing the smart coating's corrosion protection efficacy. Field Emission Scanning Electron Microscopy (FESEM) examined the coating's morphology, while Energy-Dispersive X-ray Spectroscopy (EDX) provided elemental composition data. A particle size analyser measured the size distribution of BTA-HNT and MCs, offering insights into particle sizes with different mixing techniques. This analysis involved dispersing 0.05 g of BTA-HNT and MCs into 150 mL of deionised water.

Characterisation of Smart Coating System

The performance of smart coating can be characterised using the Adhesion Test, Scratch Test, and EIS.

Electrochemical Impedance Spectroscopy (EIS)

EIS was used to assess the corrosion protection of carbon steel substrates coated with epoxy resin, varying concentrations of BTA-HNT, and boiled linseed oil microcapsules (MCs). Measurements were taken at open circuit potential after each 0, 7, and 14 days of immersion in a 3.5 wt% NaCl solution, applying a sinusoidal potential perturbation of 10 mV over a frequency range of 10^5 Hz to 10^{-2} Hz. This provided valuable data on impedance values and corrosion resistance. An electrochemical workstation with a working electrode, a saturated calomel reference electrode ($Hg/Hg_2Cl_2/KCl$), and a platinum counter electrode was used to obtain Bode, Nyquist, and Phase plots.

The Bode plot shows impedance magnitude (|Z|) versus frequency on a logarithmic scale which provides insights into the coating's resistance behaviour. The Nyquist plot displays the imaginary part of the impedance (-Z″) versus the real part (Z′), helping visualise the coating's resistive and capacitive properties. The Phase plot shows the phase angle (θ) of the impedance versus frequency, indicating how the coating's ability to store or release energy varies with frequency. EIS measurements replicated a corrosive environment similar to real-world conditions, providing essential insights into the coatings' performance.

Scratch Test

Scratch tests assessed the self-healing capabilities of the coatings. Controlled scratches (0.75 cm × 0.75 cm) were made on each coating, and the healing process was observed over 0, 7, and 14 days.

Adhesion Test

An adhesion test evaluated the epoxy coating's adhesion strength on a metal substrate, crucial for effective corrosion protection. Following ASTM D4541, the coating thickness should exceed 200 µm, measured by an Elcometer 456. Before testing, cylindrical metal dollies and coated sample surfaces were cleaned. Glue was applied to the dollies attached to the coated surface, and any excess glue was removed. A static load was applied while the glue set and samples were cured for 24 hours. The dollies were then vertically removed, and the force needed to dislodge them quantified the adhesion strength. The study examined how BTA-HNT and microcapsules affected the adhesion of the epoxy coating, providing essential data on bonding strength and coating performance that aligns with the study [6].

DISCUSSION

Sample Fabrication and Characterisation

The samples were successfully fabricated using magnetic stirring and sonication techniques, incorporating BTA-HNT and microcapsules into the epoxy resin. The characterisation confirmed the quality of the microcapsules and their dispersion within the coatings.

Characterisation of the Synthesised BTA-HNT and Microcapsules

Characterisation of the Encapsulation

FTIR analysis verified the encapsulation of BTA within HNT and the successful formation of microcapsules. Key absorption peaks, as shown in Figure 4, were identified, indicating the presence of functional groups associated with BTA, HNT, and linseed oil.

In the spectrum of HNT, distinctive peaks were observed, with the O–H stretching of inner hydroxyl groups prominently appearing at approximately 3690 and 3625 cm^{-1}. The characteristic peak corresponding to the stretching vibration of adsorbed water molecules was evident around 3545 cm^{-1}. The adsorbed water molecules' O–H bending vibration manifested around

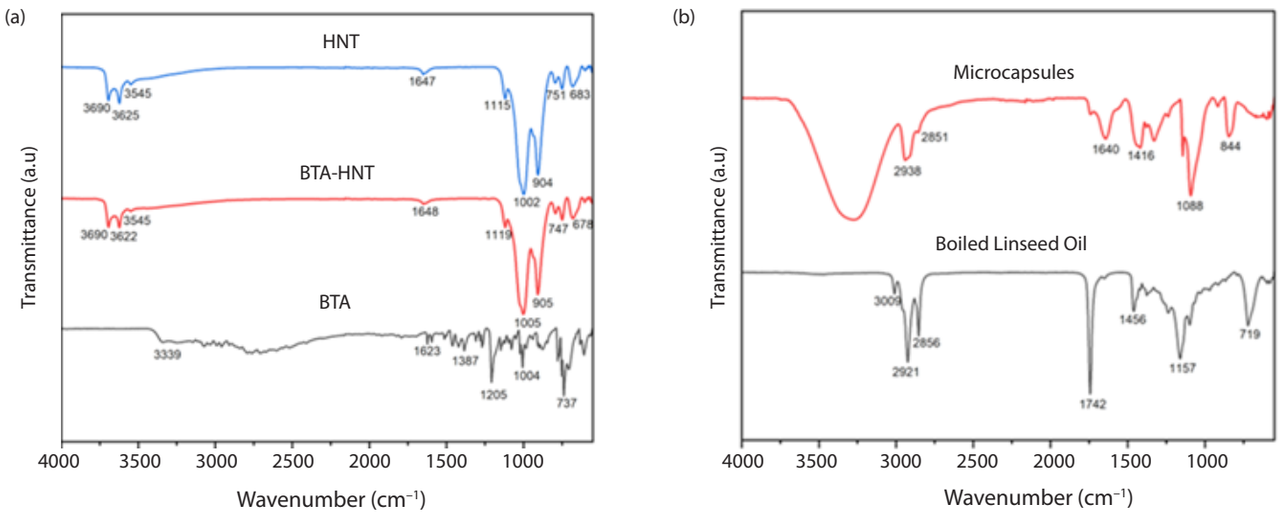

Figure 4 FTIR spectrum of (a) BTA, HNT and BTA-HNT (b) boiled linseed oil and microcapsules

1647 cm^{-1}. Additionally, absorption bands at 683 and 751 cm^{-1} were attributed to the bending vibrations of Si-O-Si and Al-O-Si, respectively. The characteristic peaks related to Si-O stretching and Al-OH bending vibrations were detected around 1115, 1002, and 904 cm^{-1}. Comparison with the FTIR spectrum of HNT-BTA revealed the presence of all aforementioned absorption peaks, indicating successful encapsulation.

The spectrum of pure linseed oil showed a prominent absorption peak around 1742 cm^{-1}, attributed to the C=O stretching vibration. Additional 1157 cm^{-1} and 1456 cm^{-1} peaks correspond to C–O stretching vibrations. Three peaks within the range of 2856-3009 cm^{-1} were associated with sp3 C–H stretching and bending vibrations, and a small shoulder in the 1600-1660 cm^{-1} range was linked to C=C stretching vibrations. These spectral features confirmed the successful synthesis of the microcapsules.

Loading Efficiency

EDX result, as illustrated in Figure 5, confirmed the loading of BTA onto HNTs. The presence of oxygen, aluminium, and silica, along with carbon and oxygen from linseed oil, validated the incorporation of BTA-HNT microcapsules within the coatings. Copper peaks indicated successful Cu loading at the ends of the HNTs. The error (σ) in the EDX spectra data for all readings is close to 0, indicating that the results obtained are reliable for interpretation.

Particle Size Distribution

The particle size distribution of synthesised BTA-HNT and MCs was analysed using a laser scattering particle size distribution analyser, with results shown in Table 2 and Figure 6. Sonication proved more effective than stirring in achieving finer and more uniform particles, supported by Zahidah et al. [29]. Key parameters indicate that sonication yields smaller D10, D50, and D90 values. D10 represents the size below which 10% of particles fall, D50 is the median size, and D90 is the size below which 90% of particles are found. The finer particle sizes achieved with sonication contribute to better dispersion and enhanced coating performance.

Table 2 Mean size and surface area of BTA-HNT and MCs

Sample	Mean Size [μm]	Surface Area [cm^2/cm^3]
Sonication of BTA-HNT	14.28975	92075
Stirring of BTA-HNT	17.92111	6546.3
Sonication of Microcapsules	405.76541	2.1671 × 105
Stirring of Microcapsules	534.12799	181.73

Coating Procedure

Metal surface preparation

The sandblasting process effectively removed rust and contaminants from the carbon steel surfaces, providing a clean substrate for coating application.

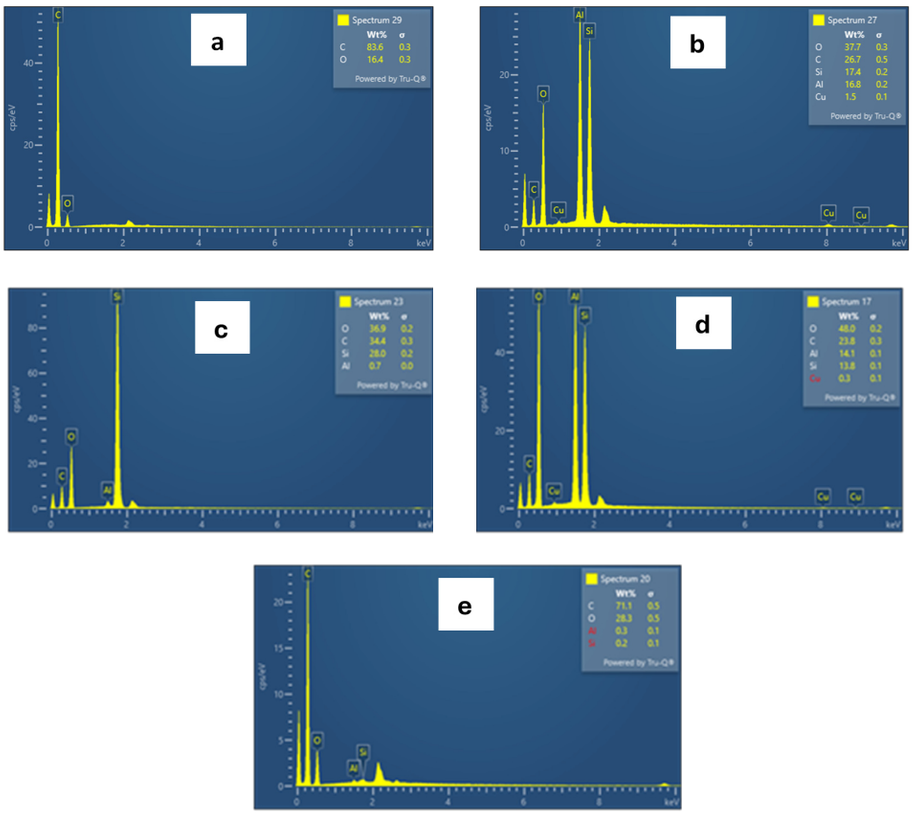

Figure 5 EDX analysis for coating of (a) EP (b) 0.1 St (c) 0.15 St (d) 0.15 Sn (e) 0.2 St

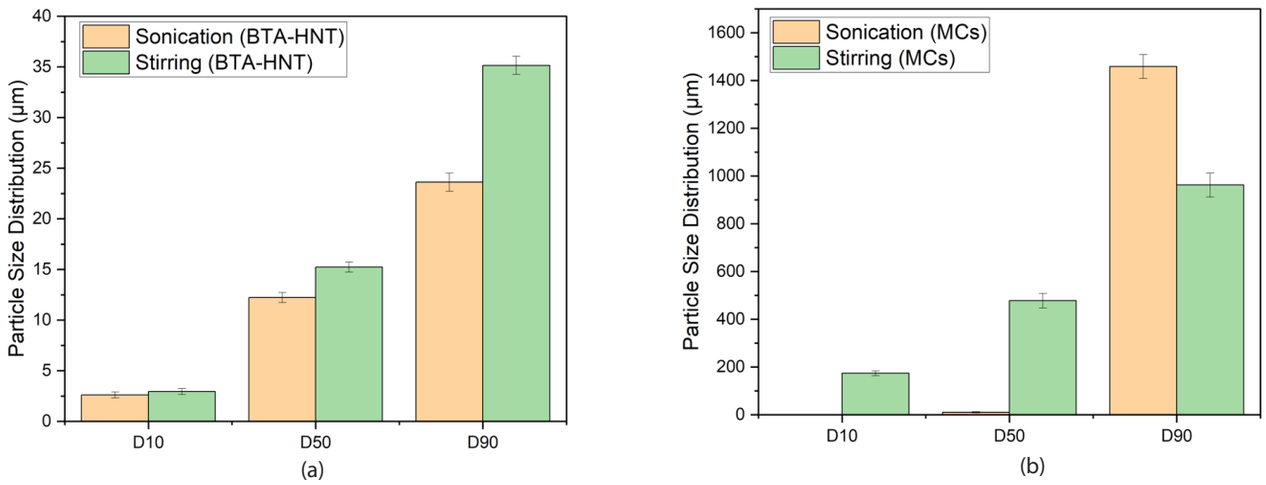

Figure 6 Particle size distribution of (a) BTA-HNT (b) microcapsules

Preparation and Characterisation of Smart Coating

Epoxy and smart coatings with various BTA-HNT and microcapsule concentrations were prepared using different mixing techniques and observed under an optical microscope, as shown in Figure 6. Proper dispersion of BTA-HNT and microcapsules in the epoxy is crucial for effective self-healing. The OM images confirm that each coating achieved even dispersion.

Based on Figure 7, the coating of 0.1 St showed a relatively uniform dispersion with minimal aggregation of BTA-HNT and fewer microcapsules (MCs). The green

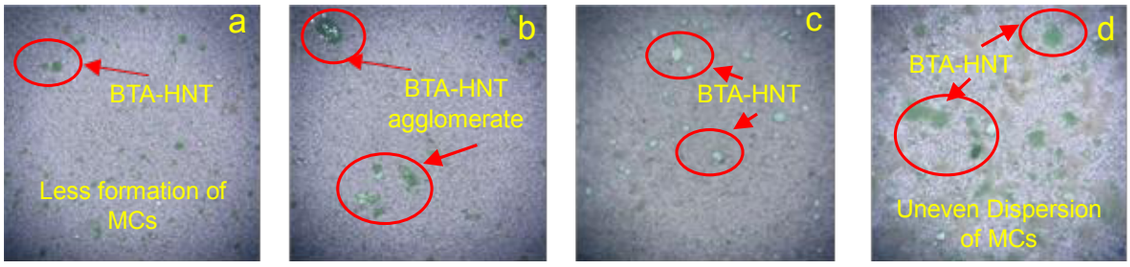

Figure 7 OM images of the smart coating (a) 0.1 St (b) 0.15 St (c) 0.15 Sn (d) 0.2 St

BTA-HNT particles are evenly distributed, indicating a good level of dispersion. In contrast, increasing the concentration to 0.15 wt% with the same stirring method resulted in more noticeable clustering and less uniformity of BTA-HNT, as shown in Figure 7b. This is due to the formation of BTA-HNT agglomerates. In the case of 0.15 Sn, the coating exhibited a finer and more even distribution of particles, demonstrating the efficacy of sonication in achieving better dispersion at higher concentrations. The particles are less aggregated, showing an effective use of sonication in maintaining uniform distribution. The white-grey microcapsules are also more uniformly distributed compared to the other samples.

The highest concentration of 0.2 St led to significant aggregation and uneven dispersion of BTA-HNT and MCs, as indicated in Figure 7d. A higher concentration of green BTA-HNT particles and more white-grey microcapsules indicate poor dispersion. The uneven distribution highlights the limitations of stirring for maintaining uniformity at elevated concentrations. This aligns with the study of Liu et al. [8], emphasising the need for enhanced dispersion techniques at higher concentrations.

Morphological Structure

The morphology of smart coatings with varying concentrations of BTA-loaded HNT and microcapsules of boiled linseed oil was examined using FESEM. Figure 8 shows the FESEM images at 20000X magnification, revealing differences in surface textures based on the concentrations and incorporation methods of BTA-HNT and microcapsules.

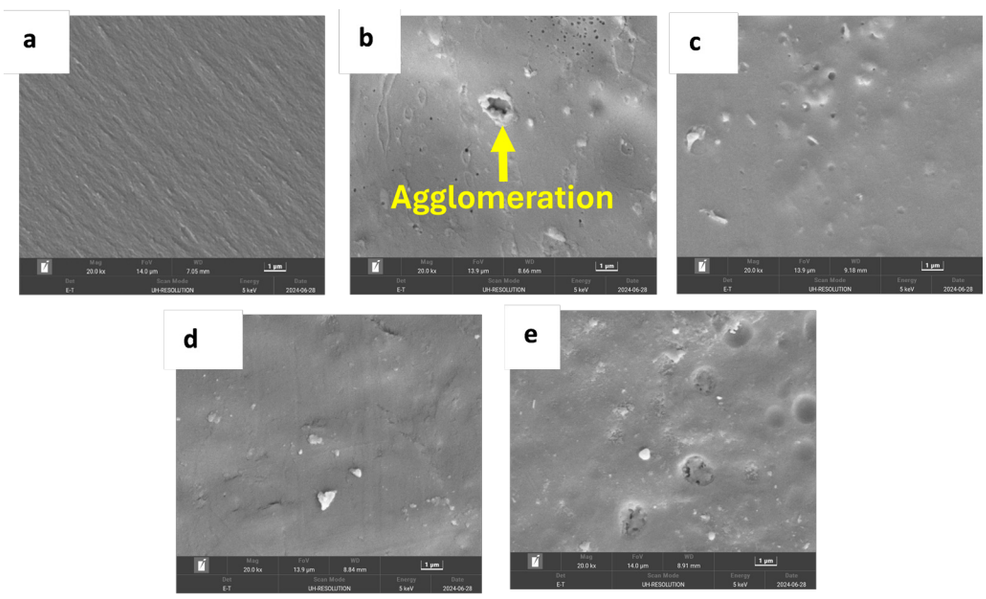

Figure 8 FESEM images for coating of (a) EP (b) 0.1 St (c) 0.15 St (c) 0.15 Sn (e) 0.2 St

Based on Figure 8, the EP coating presented a smooth surface typical of a basic epoxy coating devoid of any additives. The surface roughness and feature density increased with the inclusion of 10 wt% to 20 wt% BTA-HNT and microcapsules, displaying more pronounced particle embeddings and apparent microcapsule formations. Notably, 0.15 Sn showed a smoother surface than those prepared via stirring, indicating more effective dispersion of the additives. However, 0.2 St revealed a significantly textured surface, indicating challenges in achieving uniform dispersion. These differences underscore the substantial impact of additive concentration and preparation techniques on the microstructural properties of the coatings.

Characterisation of Coating Performance

Electrochemical Impedance Spectroscopy (EIS)

To assess the self-repairing and anti-corrosion abilities of the coatings, as well as the impact of varying microcapsule concentrations, scratched coatings were immersed in a 3.5% NaCl solution at room temperature for 14 days, followed by continuous EIS tests. As the immersion time increased, electrolyte permeation led to a decrease in impedance modulus. A higher impedance modulus at 0.01 Hz indicates better corrosion resistance.

The bode plots for the self-healing coating samples with 0.1 St, 0.15 St, 0.15 Sn, and 0.2 St are shown in

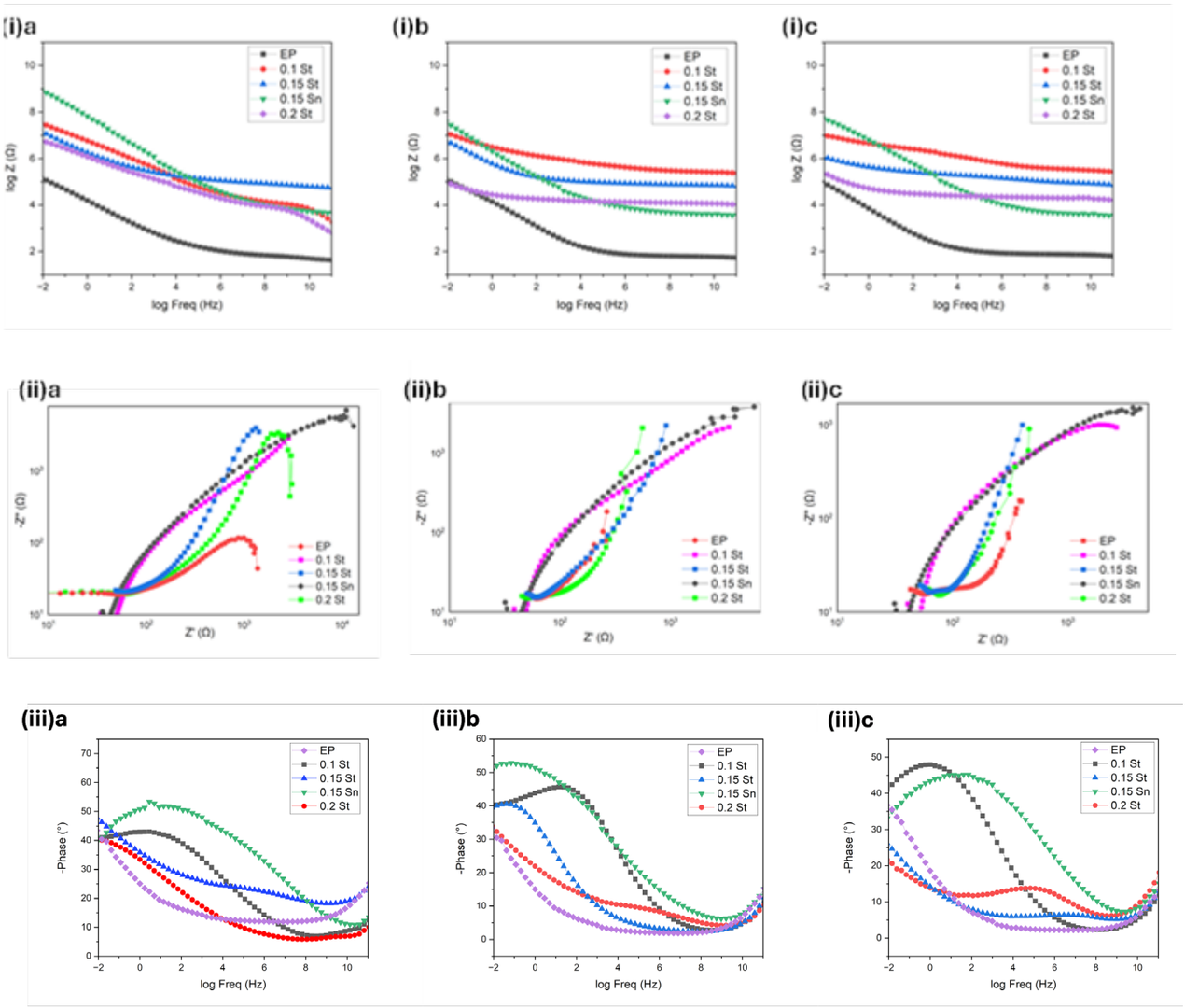

Figure 9 (i) Bode (ii) Nyquist and (iii) Phase plots of smart coating for (a) Day 0 (b) Day 7 (c) Day 14

Figures 9ia to 9ic. On Day 0, the impedance at 0.01 Hz for the 0.1 St coating was $10^8\Omega$; for 0.15 St, it was 107 Ω; for 0.15 Sn, it was 109 Ω; and for 0.2 St, it was 10^7 Ω. The EP coating (control) showed the lowest initial impedance at 10^5 Ω. Over the immersion period, the impedance values decreased, indicating a reduction in corrosion resistance as the electrolyte permeated the coatings. By Day 14, the impedance of the 0.1 St coating decreased to 10^7 Ω, 0.15 St to 10^6 Ω, 0.15 Sn to 10^8 Ω, and 0.2 St to 10^5 Ω, while the EP coating further decreased to 10^4 Ω.

These results indicate that the 0.15 Sn coating, prepared using the sonication technique, demonstrated the highest and most stable impedance values over the 14 days, suggesting superior long-term corrosion protection. The particle size analyser results show the effective dispersion of BTA-HNT and microcapsules

Table 3 OM images of the scratch area after immersion for 0,7 and 14 days

Sample	Day 0	Day 7	Day 14
EP	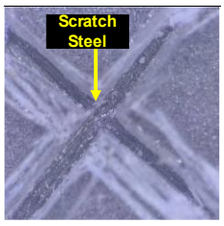	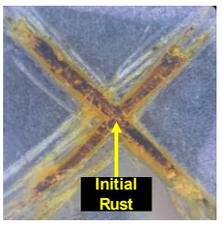	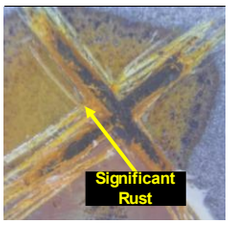
0.1 St	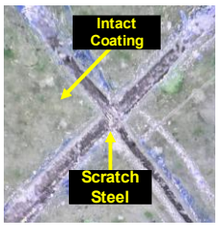	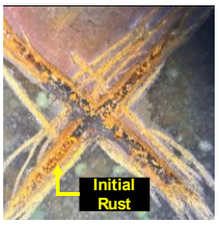	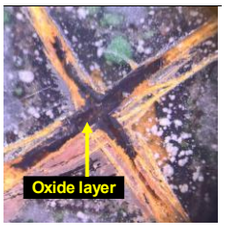
0.15 St	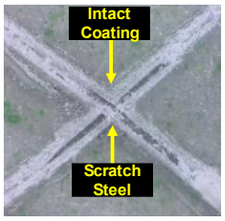	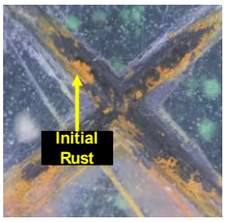	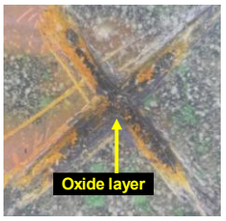
0.15 Sn	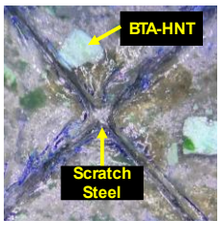	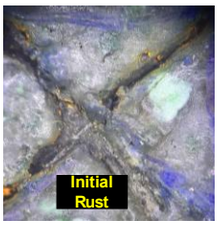	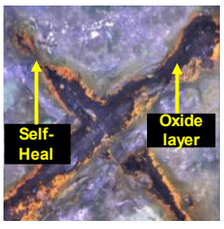
0.2 St	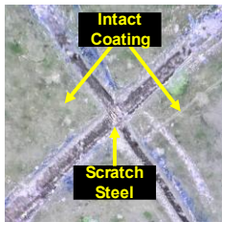	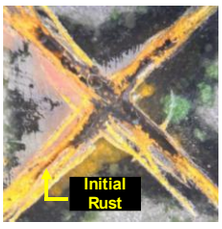	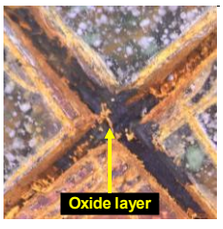

in the 0.15 Sn coating, contributing to its enhanced self-healing and anti-corrosion properties. In contrast, the coatings prepared with magnetic stirring (0.1 St, 0.15 St, and 0.2 St) showed lower impedance values and less effective performance.

The observed results aligned with the changes in capacitive arcs depicted in the Nyquist plots shown in Figures 9iia to 9iic, where the diameters of these arcs expanded for self-healing coatings incorporating BTA-HNT and microcapsules at 0 days of immersion and then gradually contracted as immersion duration increased. A similar trend was noted in the phase angle data, as shown in Figures 9iiia to 9iiic. These results indicated that 0.15 Sn had the optimal self-healing and anti-corrosion properties. In terms of coatings prepared under stirring techniques, 0.1 St had better corrosion resistance compared to 0.15 St and 0.2 St. The coating with 0.15 Sn exhibited the largest capacitive arc diameter.

Scratch Test

Scratch tests in Table 3 revealed that coatings with 15 wt% BTA-HNT and microcapsules prepared using sonication effectively sealed scratches over 14 days.

Table 3 shows the protective effects of epoxy coatings with different concentrations of BTA-HNT and microcapsules on carbon steel over 0, 7, and 14 days. The epoxy coating without additives (EP) showed significant rust by Day 7 and extensive corrosion by Day 14, indicating poor protection due to electrolyte penetration and accumulation of corrosion byproducts. The 0.1 St coating showed minimal rust and a significant oxide layer, while the 0.15 St and 0.2 St coatings exhibited moderate rust and partial oxide layers, suggesting 10 wt% is optimal for stirring techniques. The 0.15 Sn coating performed best, with minimal rust and excellent self-healing observed on both Day 7 and Day 14, due to better microcapsule dispersion from sonication. Thus, 10 wt% is optimal for stirring, while 15 wt% with sonication offers superior corrosion resistance and self-healing.

Adhesion Test

Effective adhesion is crucial for coatings to protect surfaces from corrosion. The addition of BTA-HNT and MCs to epoxy coatings was evaluated using pull-off tests. Zhang et al. [14] found that microcapsules can decrease adhesion strength due to interface defects.

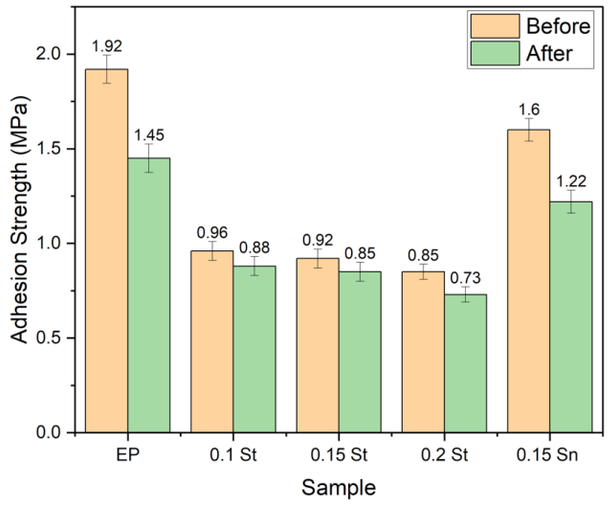

Figure 10 Adhesion strength of epoxy and smart coating before and after immersion

Figure 10 shows that adhesion strength varies with the concentration of BTA-HNT and MCs and the mixing techniques used. After immersion in NaCl, all coatings showed reduced adhesion strength. Higher concentrations generally reduced adhesion strength due to aggregation, except in sonicated samples. Sonication produced microcapsules with smoother surfaces and more uniform sizes, enhancing adhesion. The control epoxy (EP) had the highest adhesion strength, as it remained undisturbed by particles. In contrast, 0.2 St had the lowest adhesion strength of 0.82 MPa due to excessive concentration causing aggregation and weak bonding.

CONCLUSION

This study examined the effectiveness of smart coatings containing BTA-HNT and boiled linseed oil microcapsules (MCs) in enhancing the anti-corrosive and self-healing properties of epoxy coatings on carbon steel. Coatings with 10-wt% BTA-HNT and MCs formulated using the magnetic stirring method provided good corrosion protection. At the same time, those containing 15-wt% BTA-HNT and MCs sonicated showed better performance, including better particle dispersion, mechanical strength and better self-healing capabilities. Electrochemical Impedance Spectroscopy (EIS) and scratch tests confirmed the superior long-term protection of the sonicated samples, with higher impedance values sustained over 14 days. The results highlight the significance of microcapsule

concentration and preparation method in optimising self-healing epoxy coatings. Future work should involve field testing to evaluate the coatings' durability under real-world conditions, exploring different microcapsule concentrations, and integrating other corrosion inhibitors to enhance coating performance and scalability for industrial use.

ACKNOWLEDGEMENT

The authors extend their heartfelt appreciation to the Department of Material Engineering faculty members at Universiti Teknologi Petronas for providing the opportunity to contribute to this project. This research was supported by funding from Yayasan Universiti Teknologi PETRONAS (YUTP) under cost centre 015LC0-519.

REFERENCES

[1] T. E. Perez, "Corrosion in the Oil and Gas Industry: An Increasing Challenge for Materials," *Journal of The Minerals, Metals & Materials Society*, vol. 65, no. 8, pp. 1033-1042, 2013.

[2] J. Li, Z. Li, Q. Feng, H. Qiu, G. Yang, S. Zheng, and J. Yang, "Encapsulation of linseed oil in graphene oxide shells for preparation of self-healing composite coatings," *Progress in Organic Coatings*, vol. 129, pp. 285-291, 2019, doi: https://doi.org/10.1016/j.porgcoat.2019.01.024.

[3] D. Xu, C. Lou, J. Huang, X. Lu, Z. Xin, and C. Zhou, "Effect of inhibitor-loaded halloysite nanotubes on active corrosion protection of polybenzoxazine coatings on mild steel," *Progress in Organic Coatings,* vol. 134, pp. 126-133, 2019, doi: https://doi.org/10.1016/j.porgcoat.2019.04.021.

[4] X. Zhu, Q. Li, L. Wang, W. Wang, S. Liu, C. Wang, Z. Xu, L. Liu, and X. Qian, "Current advances of Polyurethane/Graphene composites and its prospects in synthetic leather: A review," *European Polymer Journal,* vol. 161, p. 110837, 2021, doi: https://doi.org/10.1016/j.eurpolymj.2021.110837.

[5] A. Ebrahiminiya, M. Khorram, S. Hassanajili, and M. Javidi, "Modeling and optimisation of the parameters affecting the in-situ microencapsulation process for producing epoxy-based self-healing anti-corrosion coatings," *Particuology*, vol. 36, pp. 59-69, 2018, doi: https://doi.org/10.1016/j.partic.2017.01.010.

[6] G. Kurt Çömlekçi and S. Ulutan, "Acquired self-healing ability of an epoxy coating through microcapsules having linseed oil and its alkyd," *Progress in Organic Coatings*, vol. 129, pp. 292-299, 2019, doi: https://doi.org/10.1016/j.porgcoat.2019.01.022.

[7] X. Fu, W. Du, H. Dou, Y. Fan, J. Xu, L. Tian, J. Zhao, and L. Ren, "Nanofiber Composite Coating with Self-Healing and Active Anti-corrosive Performances," *ACS Applied Materials & Interfaces*, vol. 13, no. 48, pp. 57880-57892, 2021, doi: 10.1021/acsami.1c16052.

[8] S. Hasnain and S. H. Ali Pirzada, *Corrosion in Oil and Gas Industries: A Review*, 2022.

[9] N. C. M. Spera, C. Salazar-Castro, P. C. Álvarez de Eulate, Y. V. Kolen'ko, and J. P. S. Sousa , "Self–healing core–shell nanofibers for corrosion protective coatings for offshore structures," *Progress in Organic Coatings,* vol. 191, p. 108424, 2024, doi: https://doi.org/10.1016/j.porgcoat.2024.108424.

[10] N. A. bin Mohd Hamidi, W. Ikhmal, N. Nasir, M. S. Shaifudin, and M. Ghazali, "Potential Application of Plant-Based Derivatives as Green Components in Functional Coatings: A Review," *Cleaner Materials*, vol. 4, p. 100097, 2022, doi: 10.1016/j.clema.2022.100097.

[11] C. Fu, A. Liu, Y. Zhai, H. Lan, S. Cui, T. Qi, and J.-P. Wang, "A smart platform for monitoring the whole life-course of self-healing coatings with the cooperation of self-reporting microcapsules and coating matrix," *Colloids and Surfaces A: Physicochemical and Engineering Aspects*, vol. 684, p. 133152, 2024, doi: https://doi.org/10.1016/j.colsurfa.2024.133152.

[12] R. Patra, A. Gautam, K. Gobi, and R. Subasri, "Hybrid Silane Coatings Based on Benzotriazole Loaded Aluminosilicate Nanotubes for Corrosion Protection of Mild Steel," *Silicon,* vol. 15, pp. 1-16, 2023, doi: 10.1007/s12633-023-02556-7.

[13] D. Li, B. Gong, Y. Liu, and Z. Dang, "Self-healing coatings based on PropS-SH and pH-responsive HNT-BTA nanoparticles for inhibition of pyrite oxidation to control acid mine drainage," *Chemical Engineering Journal,* vol. 415, p. 128993, 2021, doi: https://doi.org/10.1016/j.cej.2021.128993.

[14] D. I. Njoku, A. C. Njoku, I. I. Udoh, P. C. Uzoma, I.-I. N. Etim, B. Li, and Y. Li , "Understanding the multifunctional anti-corrosion protective mechanism of epoxy-based coatings modified with hydrogel and benzotriazole

conveying nanotubes for Q235 steel protection in 3.5 % NaCl," *Surface and Coatings Technology,* vol. 484, p. 130851, 2024, doi: https://doi.org/10.1016/j.surfcoat.2024.130851.

[15] M. Sun, A. Yerokhin, M. Y. Bychkova, D. V. Shtansky, E. A. Levashov, and A. Matthews, "Self-healing plasma electrolytic oxidation coatings doped with benzotriazole loaded halloysite nanotubes on AM50 magnesium alloy," *Corrosion Science,* vol. 111, pp. 753-769, 2016, doi: https://doi.org/10.1016/j.corsci.2016.06.016.

[16] H. H. Zhang, X. Zhang, H. Bian, L. Zhang, Y. Chen, Y. Yang, and Z. Zhang, "Benzotriazole loaded CeO2 nano-containers towards superior anti-corrosive silane coating for protection of copper," *Colloids and Surfaces A: Physicochemical and Engineering Aspects,* vol. 682, p. 132844, 2024, doi: https://doi.org/10.1016/j.colsurfa.2023.132844.

[17] E. Abdullayev and Y. Lvov, "Clay nanotubes for corrosion inhibitor encapsulation: Release control with end stoppers," *J. Mater. Chem.,* vol. 20, pp. 6681-6687, 2010, doi: 10.1039/C0JM00810A.

[18] K. A. Zahidah, S. Kakooei, M. C. Ismail, and P. Bothi Raja, "Halloysite nanotubes as nanocontainer for smart coating application: A review," *Progress in Organic Coatings,* vol. 111, pp. 175-185, 2017, doi: https://doi.org/10.1016/j.porgcoat.2017.05.018.

[19] H. Yang, Q. Mo, W. Z. Li, and F. Gu, "Preparation and Properties of Self-Healing and Self-Lubricating Epoxy Coatings with Polyurethane Microcapsules Containing Bifunctional Linseed Oil," *Polymers,* vol. 11, p. 1578, 2019, doi: 10.3390/polym11101578.

[20] D. G. Shchukin, "Container-based multifunctional self-healing polymer coatings," *Polymer Chemistry,* vol. 4, no. 18, pp. 4871-4877, 2013, doi: 10.1039/C3PY00082F.

[21] Y. Huang, C. Zhao, Y. Li, C. Wang, T. Shen, C. Wu, and H. Yang, "Enhanced corrosion resistance and self-healing effect of sol-gel coating incorporating one-pot-synthesised corrosion inhibitor-encapsulated silica nanocontainers," *Journal of Sol-Gel Science and Technology,* vol. 104, 2022, doi: 10.1007/s10971-022-05929-3.

[22] M. R. Karampoor, M. Atapour, and A. Bahrami, "Preparation of an anti-bacterial CuO-containing polyurea-formaldehyde/linseed oil self-healing coating," *Progress in Organic Coatings,* vol. 184, p. 107879, 2023, doi: https://doi.org/10.1016/j.porgcoat.2023.107879.

[23] M. Hasanzadeh, M. Shahidi, and M. Kazemipour, "Application of EIS and EN techniques to investigate the self-healing ability of coatings based on microcapsules filled with linseed oil and CeO2 nanoparticles," *Progress in Organic Coatings,* vol. 80, pp. 106-119, 2015, doi: https://doi.org/10.1016/j.porgcoat.2014.12.002. [24] T. Liu, Y. Zhao, Y. Deng, and H. Ge, "Preparation of fully epoxy resin microcapsules and their application in self-healing epoxy anti-corrosion coatings," *Progress in Organic Coatings,* vol. 188, p. 108247, 2024, doi: https://doi.org/10.1016/j.porgcoat.2024.108247.

[25] A. G. Cordeiro Neto, A. C. Pellanda, A. R. de Carvalho Jorge, J. B. Floriano, and M. A. Coelho Berton, "Preparation and evaluation of corrosion resistance of a self-healing alkyd coating based on microcapsules containing Tung oil," *Progress in Organic Coatings,* vol. 147, p. 105874, 2020, doi: https://doi.org/10.1016/j.porgcoat.2020.105874.

[26] M. Behzadnasab, S. M. Mirabedini, M. Esfandeh, and R. R. Farnood, "Evaluation of corrosion performance of a self-healing epoxy-based coating containing linseed oil-filled microcapsules via electrochemical impedance spectroscopy," *Progress in Organic Coatings,* vol. 105, pp. 212-224, 2017, doi: https://doi.org/10.1016/j.porgcoat.2017.01.006.

[27] S. M. Mirabedini, M. Esfandeh, R. R. Farnood, and P. Rajabi, "Amino-silane surface modification of urea-formaldehyde microcapsules containing linseed oil for improved epoxy matrix compatibility. Part I: Optimising silane treatment conditions," *Progress in Organic Coatings,* vol. 136, p. 105242, 2019, doi: https://doi.org/10.1016/j.porgcoat.2019.105242.

[28] D. Li, B. Gong, Y. Liu, and Z. Dang, "Self-healing coatings based on PropS-SH and pH-responsive HNT-BTA nanoparticles for inhibition of pyrite oxidation to control acid mine drainage," *Chemical Engineering Journal,* vol. 415, p. 128993, 2021, doi: https://doi.org/10.1016/j.cej.2021.128993.